Fluid-structure interactions with numerics for a smoothed augmented Lagrangian variational principle applied to a wave-energy device

Onno Bokhove, School of Mathematics, Leeds Institute for Fluid Dynamics, Leeds, UK

Sharing is encouraged

Introduction –Objective and FSI/Discretisation Strategy

Objective: We formulated, implemented & tested intriguing novel fluid-structure interaction (FSI) strategy for new wave-energy device with wave-buoy & buoy-generator interactions based on inequality constraints & Averaged Vector Field energy conservation. Used tedious bouncing ball model as pedagogically toy test. In five clear steps, our ***novel discretisation strategy*** is:

- S1: Write down the augmented Lagrangian with the inequality constraint embedded and derive the dynamics. *Why?* Includes all dynamics in one VP, directly with cunning coupling.
- S2: Approximate the Lagrange multiplier λ using new (implicit) function approximations to $\tilde{F}_+(\cdot)$, to solve for $\lambda(G) \le 0$ in terms of constraint $G \ge 0$. *Why?* Dynamics is stiff & geometric integrators perform poorly with (well-)known explicit functions $\lambda(G)$.
- S3: Write down new Lagrangian/Hamiltonian dynamics with λ eliminated. *Why?* Simpler & smoothed.
- S4: Use Average Vector Field energy (AVF) conservation as time integrator. *Why?* Working best to date. Symplectic integration failed.
- S5: Test! Derive/Obtain nonlinear solver stability criterion for Δt. *Why?* Get a handle on time-step size & convergence.

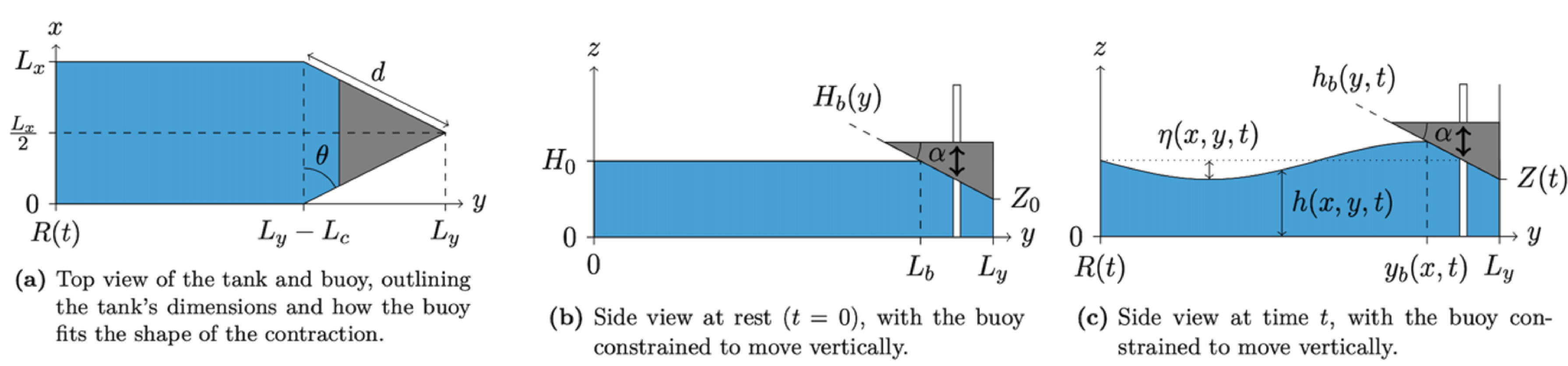

Figure 1. Sketches wave-energy device, buoy $h_B(Z(t), y)$. Courtesy Jonathon Bolton (dissertation in preparation).

S1,2,3: Models with inequality constraints

S1: Consider ***bouncing ball*** moving in vertical under constant gravity above $Z(t) \ge 0$, time t. It bounces with instant momentum reversal off the table. Augmented variational principle (VP) [2]:

$$0 = \delta \mathcal{L}_B[Z, W, \lambda] \equiv \delta \int_0^T W\,\dot{Z} - \frac{1}{2}W^2 - Z - \frac{1}{2\gamma}\left(F_+(-\gamma Z - \lambda)^2 - \lambda^2\right)\mathrm{d}t \quad (1)$$

with $\dot{Z} \equiv \mathrm{d}Z/\mathrm{d}t$, particle velocity $W(t)$, Lagrange multiplier $\lambda(t)$, constant $\gamma \gg 0$, and (maximum) function $F_+(Q) \equiv \max(0, Q)$ with $-Z \le 0$. Karush-Kuhn-Tucker (KKT) inequalities result from (2b): $-Z \le 0, \quad \lambda \le 0, \quad \lambda G(Z) = \lambda Z = 0$. Variations of (1) subject to $\delta Z(0) = \delta Z(T) = 0$ yield:

$$\delta W: \dot{Z} = W = \frac{\partial H}{\partial W}, \qquad \delta Z: \dot{W} = -\frac{\partial H}{\partial Z} = -1 + \tilde{F}_+(-\gamma Z - \lambda) = -1 - \lambda \quad (2a)$$

$$\delta\lambda: \quad \lambda = -\tilde{F}_+(-\gamma Z - \lambda) \quad \text{with} \quad \tilde{F}_+(Q) = F_+(Q)F'_+(Q) = \max(0, Q). \quad (2b)$$

S2: Seek implicit and explicit approximations of $\lambda, \tilde{F}(Q), \tilde{F}(Q)$ to enforce stability ($0 < b, d \ll 1$):

$$\text{Smooth}: \lambda_1(Z) \approx -ae^{-\gamma Z/b} = -\tilde{F}_+(Q = -\gamma Z - \lambda), Q = b\ln(\tilde{F}_+(Q)/a) + \tilde{F}_+(Q) \quad (3a)$$

$$\text{Cut-off}: \lambda_2(Z) \approx \min(0, \frac{Z}{b}), \tilde{F}_+(Q) = \frac{\max(0, Q)}{1 + b\gamma}, \quad F_+(Q) = \frac{1}{\sqrt{1 + b\gamma}}\max(0, Q) \quad (3b)$$

$$\text{Asymp.}: \lambda_3(Z) \approx a\min\left(0, \frac{Z}{b} + \frac{Z|Z|}{d}\right), \tilde{F}_+(Q) = \max\left(0, Q + \frac{(d\Gamma - d\sqrt{\Gamma^2 + 4aQ/d})}{2a/\gamma}\right) \quad (3c)$$

$$C_2: \lambda_4(Z) \approx a\left\{\frac{Z}{b}, P(Z;\delta), 0\right\} \quad \text{with} \quad P(Z) \in C_2\text{–spline}, \tilde{F}(Q), F(Q) \text{ implicit}, \quad (3d)$$

with regions $\{Z \le -\delta, |Z| < \delta, Z > \delta\}$. S3: The integral of these forces $\lambda_i(Z)$ ($i = 1, 2, 3, 4$) with respect to constraint variable $G = Z$ yields a potential $V_\lambda(G)$ in the augmented Lagrangian (1).

Wave-energy model

S1,S2,S3: Variational Boussinesq Model (VBM) water waves with surface velocity potential $\phi(x, y, t) = \phi_s(x, y, t)$ & depth $h(x, y, t)$ coupled to heaving buoy and power generator:

$$0 = \rho_0\delta\int_0^T\int_0^{L_x}\int_{R(t)}^{l_y(x)} \phi\,\partial_t h\,\mathrm{d}y\,\mathrm{d}x + MW\dot{Z} + (L_i I - K(Z))\dot{Q} - \mathcal{H}\,\mathrm{d}t \quad (4)$$

$$\begin{aligned}\equiv \rho_0\delta\int_0^T\int_0^{L_x}\int_{R(t)}^{l_y(x)} &\phi\partial_t h - \left(\frac{1}{2}h|\nabla\phi + h\psi\nabla h + \frac{1}{3}h^2\nabla\psi|^2 + \frac{1}{6}h^3\psi^2 + \frac{\beta}{90}h^5|\nabla\psi|^2\right)\\ &- gh(\frac{1}{2}h - H_0) - \frac{1}{2\gamma}\left(F_+(\gamma(h - h_b) - \lambda)^2 - \lambda^2\right)\mathrm{d}y\,\mathrm{d}x - \int_0^{L_x}\dot{R}\left(h\phi + \frac{1}{3}h^3\psi\right)|_{y=R}\,\mathrm{d}x\\ &+ MW\dot{Z} - \frac{1}{2}MW^2 - MgZ + (L_i I - K(Z))\dot{Q} - \frac{1}{2}L_i I^2\mathrm{d}t,\end{aligned} \quad (5)$$

via constraint $G = (h_b - h) \ge 0$, with $\mathcal{H}$ total energy, $\beta = 1$ for VBM and $\beta = 0$ for Green-Naghdi model [4]. Variation of this VBM-VP with respect to variables $\mathbf{q} \equiv \{h, \phi, \psi, Z, W, Q, I\}$ yields the system of equations for (conservative part of) the entire wave-energy device ([1]):

$$\delta\phi: \quad \partial_t h = \frac{1}{\rho_0}\frac{\delta\mathcal{H}}{\delta\phi}, \ \delta\psi: \ 0 = -\frac{1}{\rho_0}\frac{\delta\mathcal{H}}{\delta\psi}, \ \delta\lambda: \ 0 = \frac{1}{\rho_0}\frac{\delta\mathcal{H}}{\delta\lambda}, \ \delta h: \ \partial_t\phi = -\frac{1}{\rho_0}\frac{\delta\mathcal{H}}{\delta h} = -B + \lambda \approx -B + \underline{\underline{\lambda_i}} \quad (6a)$$

$$\delta W: \quad \dot{Z} = \frac{1}{M}\frac{\partial\mathcal{H}}{\partial W} = W \quad (6b)$$

$$\begin{aligned}\delta Z: \quad \dot{W} + \frac{\gamma_m}{M}G_I(Z)\dot{Q} &= -\frac{1}{M}\frac{\partial\mathcal{H}}{\partial Z} = -g + \frac{\rho_0}{M}\int_0^{L_x}\int_{R(t)}^{l_y(x)} F_+(\gamma(h - h_b))\,F'_+(\gamma(h - h_b))\,\mathrm{d}y\,\mathrm{d}x\\ &= -g - \frac{\rho_0}{M}\int_0^{L_x}\int_{R(t)}^{l_y(x)}\lambda\,\mathrm{d}y\,\mathrm{d}x \approx -g - \frac{\rho_0}{M}\int_0^{L_x}\int_{R(t)}^{l_y(x)}\underline{\underline{\lambda_i}}\,\mathrm{d}y\,\mathrm{d}x\end{aligned} \quad (6c)$$

$$\delta I: \quad \dot{Q} = \frac{1}{L_i}\frac{\partial\mathcal{H}}{\partial I} = I, \delta Q: \quad \dot{I} - \frac{\gamma_m}{L_i}G_I(Z)\dot{Z} = -\frac{1}{L_i}\frac{\partial\mathcal{H}}{\partial Q} - \underline{\mathit{dissipation}} \equiv \underline{-\frac{(R_i + R_c)}{L_i}I - \frac{I}{L_i|I|}V_s(|I|)}, \quad (6d)$$

with Bernoulli term B, added **electrical resistance/harvesting load** & λ_i–*approximation* (function of $h_B(Z(t), y) - h(x, y, t)$, cf. (3)). Nonlinear $K'(Z) \equiv G_I(Z)$ solves axi-symmetric 3D Maxwell's equations [1].

S5 testing & results: bouncing ball

Using $\lambda_3(Z)$ (3c) gives better convergence, since $F_+(Q) \to Q$ as $Q \to \infty$. Error is $O(\Delta t)^p$ with $p \approx 1$ compared with exact solution at $t \approx 3.5T$ for $a = 10, b = d = 0.1\Delta t^2, 10\Delta t^3$ (set-1, set-2).

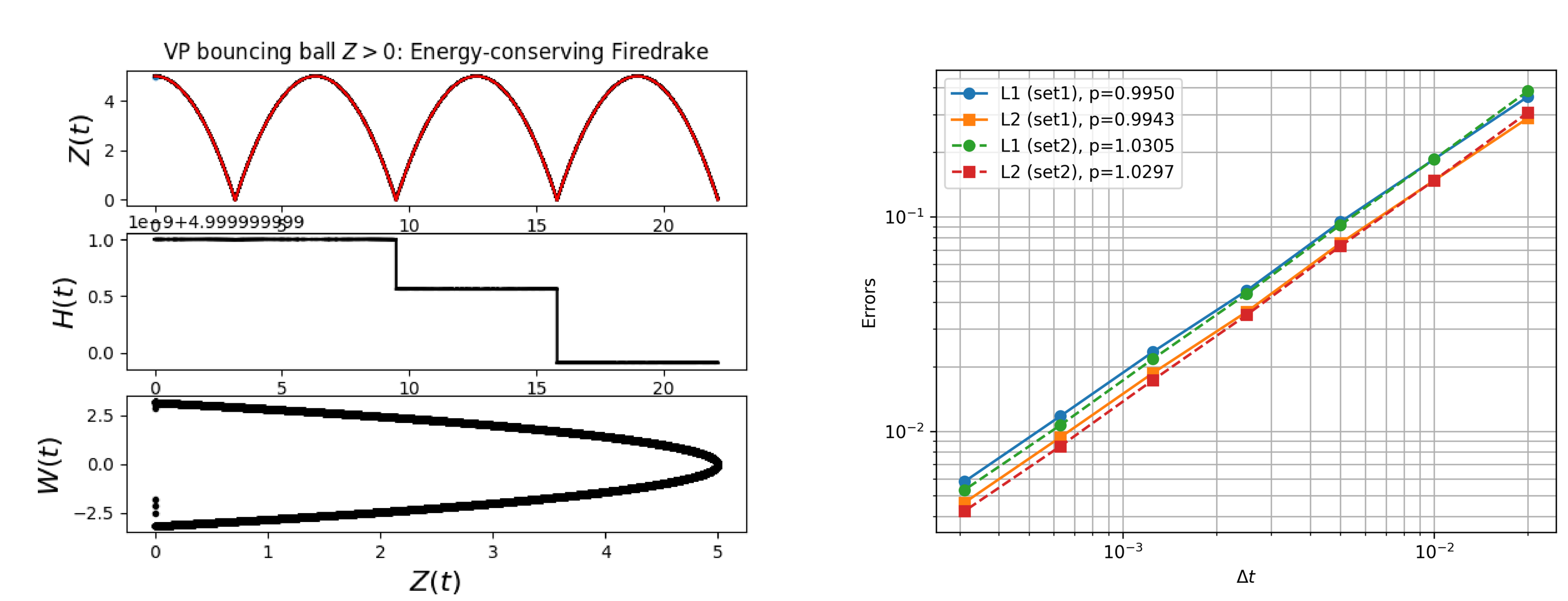

Figure 2. Left: Shown is ball under gravity bouncing off floor at $Z = 0$. Δt is not tuned. Position vs. time (exact and numerical solutions shown), energy $H(t)$ fluctuation $\sim 10^{-9}$ around $H_0 = 5$ and phase diagram $\{Z^n, W^n\}$ of numerics. Right: errors; finest errors are L_1-norm: $(0.00582, 0.00532)$ & L_2-norm: $(0.00464, 0.00424)$ at $\Delta t = 0.00031$.

Singularities in AVF have to be dealt with exactly for stability & accuracy, i.e. in Newton iterations:

$$\frac{(W^{n+1} - W^n)}{\Delta t} = -1 - a\left(\frac{(Z_-^{n+1} + Z_-^n)}{2b} - \frac{(Z_-^{n+1^2} + Z_-^{n+1}Z_-^n + Z_-^{n^2})}{3d}\right)\begin{cases}1 & Z^{n+1} = Z^n\\ \frac{Z_-^{n+1} - Z_-^n}{Z^{n+1} - Z^n} & \text{else}\end{cases}.$$

S4 AVF energy-conservation strategy

Spectrally accurate Continuous Galerkin (CG) finite element methods were used in space (e.g., 2^{nd} order CG1, CG2, CG3) with time-efficient & error-reducing automatation via & implemented in *Firedrake* environment [5]. Key take-away is that energy conserving 2^{nd}-order AVF discretisation had to be used for stability, over time $t \in [t^n, t^{n+1} = t^n + \Delta t]$. Hence, we use linear-in-s variables $\mathbf{q}(s) \equiv \big(Z(s) = (Z^n + s(Z^{n+1} - Z^n), W(s)\big)$ & likewise for $\mathbf{q}(s) \equiv \{h(x, y, s), \phi(x, y, s), \psi(x, y, s), Z(s), W(s), I(s)\}$ (e.g., [3]):

$$\frac{\partial\mathbf{q}}{\partial t} = \frac{1}{\Delta t}\frac{\mathrm{d}\mathbf{q}}{\mathrm{d}s} = J(\mathbf{q}^{n+1/2})\int_0^1\frac{\partial H[\mathbf{q}(s)]}{\partial \mathrm{q}(s)}\mathrm{d}s, \quad (7)$$

with crucial exact integration. For polynomials this is automated in Firedrake and for the λ_i's this is derived/programmed due to difficult switches & limit $\mathbf{q}^{n+1} = \mathbf{q}^n$ in Newton iterations. J is skew-symmetric tensor for (2) (J constant) or (6) (J depends on $G_I(Z)$ in W, I-equations).

S5 Testing & results: wave-energy device

For our device, $\lambda_1(G)$ works poorly since exponential explodes and, hence, $\lambda_4(G)$ is best (using $a = g, b = 10\Delta t^{3/2}$). Crucial C_2 smoothness in $\lambda_{1,4}$ is needed in CG-space. λ_4 is still too noisy.

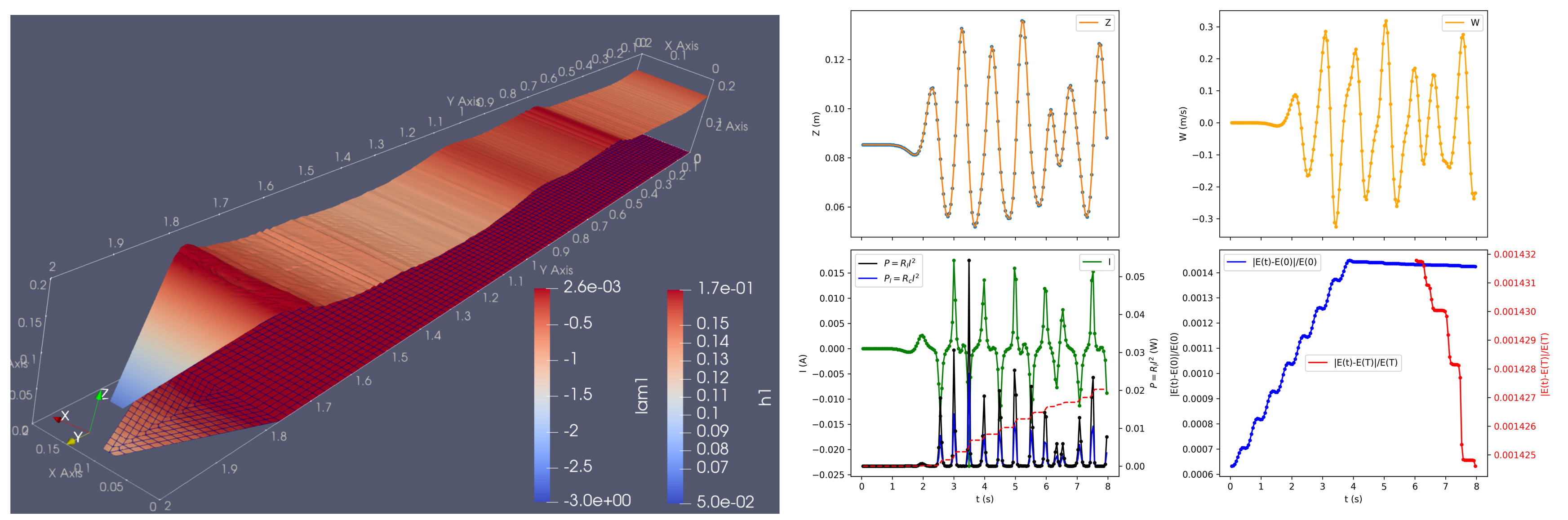

Figure 3. Left: snapshot free surface $h(x, y, t)$ & $\lambda_4(x, y, t)$ at $t = 4.08$s on mesh. Right: $Z(t), W(t), I(t)$ & harvest/circuit dissipation & scaled $\mathcal{H}(t)$ vs t. CG2 run. Post-processed λ_i still too noisy, but buoy motion & generator dynamics stable & smooth. Stable CG1–CG3 simulations completed. NB: $\delta \approx \Delta x$; buoy not shown, only its imprint.

Conclusions

The key take-aways of our new FSI-AVF framework for our new wave-energy device are:

- that singularities arising in AVF-integration, especially around the water- or contact line, need to be dealt with exactly; instant or continuous contact (C_2 needed) cases differ; and,
- that the free surface region needs to be solved exactly, i.e. have $\lambda = 0$; both work in progress.

References

[1] O. Bokhove et al. "From Bore–Soliton–Splash to a new wave-to-wire wave-energy model". In: *Water Waves* 1 (2019), pp. 217–258.

[2] E. Burman et al. "The augmented Lagrangian method ...in computational mechanics". In: *Archives Comp. Meth. Eng.* 30 (2023), pp. 2579–2604.

[3] C.J. Cotter. "Compatible FEMs for GFD". In: *Acta Numerica* 32 (2023), pp. 291–393.

[4] E. Gagarina et al. "Horizontal circulation and jumps in Hamiltonian wave models". In: *Nonl. Proc. Geophys.* 20 (2013), pp. 483–500.

[5] D. Ham et al. *Firedrake is automated system for solution of PDEs using FEM*. URL: `https://www.firedrakeproject.org/`.